Prethermalization to thermalization crossover in a dilute Bose gas following an interaction ramp

Prethermalization to thermalization crossover in a dilute Bose gas following an interaction ramp

Mathias Van Regemortel,* Hadrien Kurkjian, and Michiel Wouters
TQC, Universiteit Antwerpen, Universiteitsplein 1, B-2610 Antwerpen, Belgium

Iacopo Carusotto
INO-CNR BEC Center and Dipartimento di Fisica,
Università di Trento, via Sommarive 14, 38123 Povo, Italy
(Dated: November 22, 2018)

The dynamics of a weakly interacting Bose gas at low temperatures is close to integrable due to the approximate quadratic nature of the many-body Hamiltonian. While the short-time physics after an abrupt ramp of the interaction constant is dominated by the integrable dynamics, integrability is broken at longer times by higher-order interaction terms in the Bogoliubov Hamiltonian, in particular by Beliaev-Landau scatterings involving three quasiparticles. The two-stage relaxation process is highlighted in the evolution of local observables such as the density-density correlation function: a dephasing mechanism leads the system to a prethermal stage, followed by true thermalization conveyed by quasiparticle collisions. Our results bring the crossover from prethermalization to thermalization within reach of current experiments with ultracold atomic gases.

I. INTRODUCTION

Ever since the development of quantum mechanics in the early days, it has been a central question how the unitary time evolution of a quantum wavefunction of many particles may generate a seemingly thermal ensemble in the long-time limit – at least in the eyes of an experimenter with limited tools to probe the system. The *eigenstate thermalization hypothesis* (ETH) [1, 2] aims to address this question by stating that expectation values of macroscopic observables computed with respect to a single generic eigenstate of energy E are the same as the microcanonical average around the corresponding energy. The hypothesis has been verified numerically for a wide series of chaotic quantum systems [3, 4].

Since it relies on the hypothesis of ergodicity, ETH is not expected to hold for integrable quantum systems. There, an extensive number of conserved quantities restricts the full quantum dynamics to a small subspace of the total Hilbert space, thereby preventing thermalization. The long-time states of integrable systems can still be statistically described by a stationary *generalized Gibbs ensemble* (GGE) [5], that incorporates all the conserved charges, as was recently seen in a cold atom experiment [6]. Another seminal experimental example is the quantum Newton cradle [7]. In the same spirit as ETH, a representative eigenstate of the integrable Hamiltonian can be identified based on these conserved charges, which correctly reproduces expectation values of local observables [8].

Similarly, approximate integrable systems can go through a *dephasing* stage, after which they are left in a *prethermal* state [9], also described by a GGE with all the approximately conserved quantities. Nevertheless, at longer times true thermalization sets in, conveyed by higher-order relaxation processes, such as illustrated in Fig. 1(a).

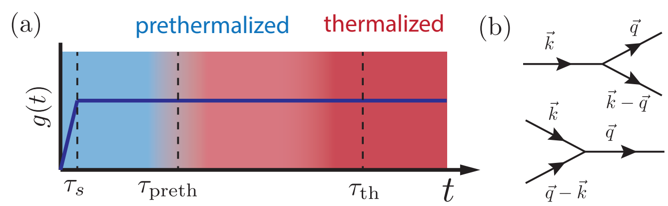

Figure 1. (a) A pictorial image of the separation of time scales considered for this work. The gas is brought out of equilibrium by abruptly ramping up the interaction constant g in a time τ_s. Then, the approximate integrability of Hamiltonian (1) leads the system through a prethermalization stage (blue shades) on a time scale $\tau_{\rm preth}$ set by the chemical potential μ. Finally, a thermal equilibrium is reached on a vastly longer time scale $\tau_{\rm th}$ through Beliaev-Landau collisions (red shades). Alternatively, the red shades can be seen as representing the growth of thermodynamic entropy. (b) Diagrams of the predominant non-integrable collisions that drive the system toward full thermalization; Beliaev decay (up) and Landau scattering (down).

II. THE HAMILTONIAN

As for now, the literature on the crossover from a prethermalized to a thermalized state after a global quench has been mostly restricted to toy models. It was studied how a 1D chain [10] or liquid [11] of spinless fermions with weak integrability breaking first relaxes to a prethermal state, after which a kinetic picture allows to understand the full thermalization dynamics of the model.

In this manuscript, we aim to bring the study of the

* Mathias.VanRegemortel@uantwerpen.be

two distinct relaxation mechanisms within the realm of current experiments. An example of an experimentally relevant system that is close to being integrable is provided by the weakly interacting Bose gas, described by the standard Hamiltonian in 3D (we use units of $\hbar = 1$)

$$\hat{H} = \sum_{\mathbf{k}} \frac{k^2}{2m} \hat{a}^\dagger_{\mathbf{k}} \hat{a}_{\mathbf{k}} + \frac{g}{2V} \sum_{\mathbf{p},\mathbf{k},\mathbf{q}} \hat{a}^\dagger_{\mathbf{p}+\mathbf{q}} \hat{a}^\dagger_{\mathbf{k}-\mathbf{q}} \hat{a}_{\mathbf{k}} \hat{a}_{\mathbf{p}}. \tag{1}$$

Here, V is the volume of the gas, m is the particle mass and g is the effective interaction constant, found from the s-wave scattering length a_s as $g = 4\pi a_s/m$.

Starting from the ground state of an ideal gas with density n, we perform an abrupt ramp of the interaction constant $g_i \to g_f$ (with $g_i = 0 < g_f$) within a nonzero time window τ_s (see Fig. 1(a)), and study the subsequent dynamics under Hamiltonian (1). Experimentally, this can be done with a Feshbach resonance [12] by suddenly ramping up an external magnetic field. Recently, this mechanism was utilized to probe the analog of cosmic Sakharov oscillations in a 2D bosonic gas [13]. In low dimensions, the interaction constant can also be modified by varying the transverse confinement [14].

When interactions are weak (small na_s^3) and well below the critical temperature, almost all particles are found in the $\mathbf{k} = 0$ mode, justifying the replacement $\hat{a}_0 \to \langle \hat{a}_0 \rangle \equiv \sqrt{n_0 V}$, where $n_0 \approx n$ is the condensate density. The dynamics of the bosonic gas after an interaction quench was studied on the level of a quadratic approximation in fluctuation operators $\mathbf{k} \neq 0$ [15, 16], and later the departure from the prethermalized state was considered [17] and the damping of the oscillations was added by hand [18].

We, however, seek to explicitly retain terms containing three fluctuation operators as well, so as to describe higher-order (non-integrable) scatterings that eventually lead the system toward thermalization. In the literature on superfluidity, these are commonly studied in the context of Beliaev decay and Landau damping [19], where they are responsible for the damping of a phonon [20–23].

By truncating (1) at third order in fluctuation operators [24], we find the approximate Hamiltonian,

$$\hat{H} \approx E_0 + \hat{H}_2 + \hat{H}_3. \tag{2}$$

The quadratic part can be diagonalized with the standard Bogoliubov transformation $\hat{a}_{\mathbf{k}} = u_k \hat{\chi}_{\mathbf{k}} + v_k \hat{\chi}^\dagger_{-\mathbf{k}}$, with

$$u_k, v_k = \pm\sqrt{\frac{k^2/2m + gn_0}{2\omega_k} \pm \frac{1}{2}}, \tag{3}$$

and the quasiparticle frequency

$$\omega_k = \sqrt{\frac{k^2}{2m}\Big(\frac{k^2}{2m} + 2gn_0\Big)}. \tag{4}$$

In terms of the Bogoliubov operators, Hamiltonian (2) is then expressed as [25]

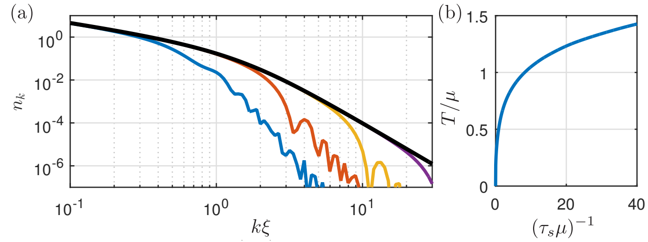

Figure 2. Effect of an interaction quench $g_i = 0 \to g_f$. (a) The momentum distribution $n^{(\chi)}_{\mathbf{k}}$ of quasiparticles after the interaction ramp for decreasing switching times $\tau_s = \{5,\ 0.5,\ 0.05,\ 0.005\} \times \mu^{-1}$; the thick black line is the limiting case $\tau_s \to 0$, for which we have result (13). $n^{(\chi)}_{\mathbf{k}}$ constitutes a conserved charge of $\hat{H}_2$ and only evolves under $\hat{H}_3$. (b) Upon decreasing switching time τ_s more energy is injected into the system, which then translates into a higher equilibrium temperature T. For $\tau_s \to 0$, we derive $T = O(\tau_s^{-1/5})$.

$$\hat{H}_2 = \sum_{\mathbf{k}} \omega_k \hat{\chi}^\dagger_{\mathbf{k}} \hat{\chi}_{\mathbf{k}}, \tag{5}$$

$$\hat{H}_3 = g\sqrt{\frac{n_0}{V}} \sum_{\mathbf{k},\mathbf{q}} \Big(A_{\mathbf{k},\mathbf{q}} \hat{\chi}^\dagger_{\mathbf{k}} \hat{\chi}^\dagger_{\mathbf{q}} \hat{\chi}_{\mathbf{k}+\mathbf{q}} + B_{\mathbf{k},\mathbf{q}} \hat{\chi}_{\mathbf{k}} \hat{\chi}_{\mathbf{q}} \hat{\chi}_{-\mathbf{k}-\mathbf{q}} + \text{h.c} \Big), \tag{6}$$

with the matrix elements of $\hat{H}_3$

$$A_{\mathbf{k},\mathbf{q}} = u_{\mathbf{k}} u_{\mathbf{q}} u_{\mathbf{k}+\mathbf{q}} + v_{\mathbf{k}} v_{\mathbf{q}} v_{\mathbf{k}+\mathbf{q}} + \big(u_{\mathbf{k}+\mathbf{q}} + v_{\mathbf{k}+\mathbf{q}}\big)\big(u_{\mathbf{k}} v_{\mathbf{q}} + u_{\mathbf{q}} v_{\mathbf{k}}\big), \tag{7}$$

$$B_{\mathbf{k},\mathbf{q}} = \frac{1}{3}\Big(u_{\mathbf{k}} u_{-\mathbf{k}-\mathbf{q}} v_{\mathbf{q}} + (u_{\mathbf{q}} + v_{\mathbf{q}})(u_{\mathbf{k}} v_{-\mathbf{k}-\mathbf{q}} + u_{-\mathbf{k}-\mathbf{q}} v_{\mathbf{k}}) + v_{\mathbf{k}} v_{-\mathbf{k}-\mathbf{q}} u_{\mathbf{q}} \Big). \tag{8}$$

Upon taking the thermodynamic limit and rescaling the wave numbers with the healing length $\xi = \sqrt{1/m\mu}$, $k \to \tilde{k} = k\xi$ one notices that the density of states times the matrix elements of $\hat{H}_3$ squared scale as $1/(n\xi^3) = \sqrt{(4\pi)^3 n a_s^3}$, exactly like the condensate depletion $n - n_0$. Therefore, if the number of depleted particles is sufficiently small, the dynamics under the integrable Hamiltonian $\hat{H}_2$ occurs on a substantially faster time scale than the ergodic dynamics of $\hat{H}_3$ [26].

III. THE EQUATIONS OF MOTION

We start by looking at the short-time dynamics, primarily generated by $\hat{H}_2$, such as studied in [15]. In particular, the interaction ramp takes place within a nonzero time window, short enough so that we can safely neglect any effects of $\hat{H}_3$ during the quench. We return to the basis of fluctuation operators and find that the dynamics of the quadratic correlation functions $n_k^{(a)} = \langle \hat{a}_{\mathbf{k}}^\dagger \hat{a}_{\mathbf{k}} \rangle$ and $c_k^{(a)} = \langle \hat{a}_{\mathbf{k}} \hat{a}_{-\mathbf{k}} \rangle$ is governed by [15]

$$\partial_t n_k^{(a)} = -2\Im\big[g(t) n_0 c_k^{(a)}\big], \tag{9}$$

$$i\partial_t c_k^{(a)} = 2\Big(\frac{k^2}{2m} + g(t)n_0\Big) c_k^{(a)} + g(t) n_0 (2n_k^{(a)} + 1). \tag{10}$$

This system of equations is readily integrated numerically for a given temporal profile $g(t)$ and with appropriate initial conditions. It has been intensely studied in the context of the dynamical Casimir effect [27], where a modulation of the interaction constant or condensate density causes a change of vacuum for the quasiparticle operators $\hat{\chi}_{\mathbf{k}}$ [14, 16, 28, 29]. The correlations of the quasiparticles, in turn, are then evaluated via (3) with the linear transform

$$n_k^{(\chi)} = (u_k^2 + v_k^2) n_k^{(a)} - 2u_k v_k \Re\big[c_k^{(a)}\big] + v_k^2, \tag{11}$$

$$c_k^{(\chi)} = u_k^2 c_k^{(a)} + v_k^2 c_k^{(a)*} - 2u_k v_k n_k^{(a)} - u_k v_k. \tag{12}$$

In the limit of instantaneous switching time $\tau_s \to 0$, we find the correlation functions after the quench as

$$n_k^{(\chi)} = v_k^2, \quad c_k^{(\chi)} = -u_k v_k. \tag{13}$$

In Fig. 2(a), we show the quasiparticle momentum distribution for different τ_s and see that it converges to (13) for shorter τ_s.

We now stick to the basis of Bogoliubov operators $\hat{\chi}_{\mathbf{k}}$. Their quadratic correlation functions evolve trivially under $\hat{H}_2$ as $n_k^{(\chi)}(t) = n_k^{(\chi)}$ and $c_k^{(\chi)}(t) = \tilde{c}_k^{(\chi)} e^{-2i\omega_k t}$, making $n_k^{(\chi)}$ and $\tilde{c}_k^{(\chi)}$ conserved quantities of $\hat{H}_2$ related to the integrable dynamics. However, on the level of the full Hamiltonian (2) they do experience a variation, predominantly under $\hat{H}_3$. Via Heisenberg's equation of motion, we derive the dynamics of correlation functions of quasiparticle operators in momentum space from (2). This way, we find for the quadratic correlations

$$\partial_t n_{\mathbf{k}}^{(\chi)} = 2g\sqrt{\frac{n_0}{V}}\Im\Big\{ \sum_{\mathbf{q}} 3B_{\mathbf{k},-\mathbf{q}} R_{\mathbf{k},\mathbf{q}}^* + 2A_{\mathbf{k},\mathbf{q}-\mathbf{k}} M_{\mathbf{q},\mathbf{k}} + A_{\mathbf{q},\mathbf{k}-\mathbf{q}} M_{\mathbf{k},\mathbf{q}}^* \Big\} \tag{14}$$

$$i\partial_t \tilde{c}_{\mathbf{k}}^{(\chi)} = 2g\sqrt{\frac{n_0}{V}} \sum_{\mathbf{q}} \Big\{ 3B_{-\mathbf{k},\mathbf{q}} M_{\mathbf{k},\mathbf{q}} + 2A_{\mathbf{k},-\mathbf{q}} M_{\mathbf{q},\mathbf{k}}^* + A_{\mathbf{q},\mathbf{k}-\mathbf{q}} R_{\mathbf{k},\mathbf{q}} \Big\} e^{2i\omega_k t}, \tag{15}$$

where we have introduced the correlation functions of three quasiparticles

$$M_{\mathbf{k},\mathbf{q}} = \Big\langle \hat{\chi}_{\mathbf{k}-\mathbf{q}}^\dagger \hat{\chi}_{\mathbf{q}}^\dagger \hat{\chi}_{\mathbf{k}} \Big\rangle, \quad R_{\mathbf{k},\mathbf{q}} = \Big\langle \hat{\chi}_{\mathbf{q}-\mathbf{k}} \hat{\chi}_{-\mathbf{q}} \hat{\chi}_{\mathbf{k}} \Big\rangle. \tag{16}$$

We next evaluate the equation of motion for the third-order correlators

$$i\partial_t M_{\mathbf{k},\mathbf{q}} = (\omega_{\mathbf{k}} - \omega_{\mathbf{q}} - \omega_{\mathbf{k}-\mathbf{q}}) M_{\mathbf{k},\mathbf{q}} + g\sqrt{\frac{n_0}{V}} F_{\mathbf{k},\mathbf{q}}^{(M)}, \tag{17}$$

$$i\partial_t R_{\mathbf{k},\mathbf{q}} = (\omega_{\mathbf{k}} + \omega_{\mathbf{q}} + \omega_{\mathbf{q}-\mathbf{k}}) R_{\mathbf{k},\mathbf{q}} + g\sqrt{\frac{n_0}{V}} F_{\mathbf{k},\mathbf{q}}^{(R)}. \tag{18}$$

In principle, a connected correlator of p operators couples to correlators of $p+1$ operators on the right-hand side, making this an ever-growing hierarchy [30]. After evaluation and factorization, we find the drive term of Eqs. (17)–(18) as

$$\begin{aligned} F_{\mathbf{k},\mathbf{q}}^{(M)} = {} & 2A_{\mathbf{k},-\mathbf{q}}\Big(c_{\mathbf{q}}^*(n_{\mathbf{k}-\mathbf{q}} - n_{\mathbf{k}}) - c_{\mathbf{k}-\mathbf{q}}^* c_{\mathbf{k}}\Big) \\ & + 2A_{\mathbf{k},\mathbf{q}-\mathbf{k}}\Big(c_{\mathbf{k}-\mathbf{q}}^*(n_{\mathbf{q}} - n_{\mathbf{k}}) - c_{\mathbf{k}} c_{\mathbf{q}}^*\Big) \\ & + 2A_{\mathbf{q},\mathbf{k}-\mathbf{q}}\Big(n_{\mathbf{k}-\mathbf{q}}(n_{\mathbf{q}} - n_{\mathbf{k}}) - n_{\mathbf{k}}(n_{\mathbf{q}} + 1)\Big) \\ & + 3B_{\mathbf{k},-\mathbf{q}}\Big(c_{\mathbf{k}-\mathbf{q}}^* c_{\mathbf{q}}^* - c_{\mathbf{k}} n_{\mathbf{k}-\mathbf{q}}\Big) \\ & + 3B_{\mathbf{k},\mathbf{q}-\mathbf{k}}\Big(c_{\mathbf{k}-\mathbf{q}}^* c_{\mathbf{q}}^* - c_{\mathbf{k}}(n_{\mathbf{q}} + 1)\Big) \\ & - 3B_{\mathbf{q},\mathbf{k}-\mathbf{q}}\, c_{\mathbf{k}}\Big(n_{\mathbf{q}} + n_{\mathbf{k}-\mathbf{q}} + 1\Big), \end{aligned} \tag{19}$$

and

$$\begin{aligned} F_{\mathbf{k},\mathbf{q}}^{(R)} = {} & 2A_{\mathbf{k},-\mathbf{q}}\Big(c_{\mathbf{k}-\mathbf{q}}(n_{\mathbf{k}} + n_{\mathbf{q}} + 1) + c_{\mathbf{k}} c_{\mathbf{q}}\Big) \\ & + 2A_{\mathbf{k},\mathbf{q}-\mathbf{k}}\Big(c_{\mathbf{q}}(n_{\mathbf{k}} + n_{\mathbf{k}-\mathbf{q}} + 1) + c_{\mathbf{k}-\mathbf{q}} c_{\mathbf{k}}\Big) \\ & + 2A_{\mathbf{q},\mathbf{k}-\mathbf{q}}\Big(c_{\mathbf{k}}(n_{\mathbf{q}} + n_{\mathbf{k}-\mathbf{q}} + 1) + c_{\mathbf{q}} c_{\mathbf{k}-\mathbf{q}}\Big) \\ & + 3B_{\mathbf{k},-\mathbf{q}}\, \Big((n_{\mathbf{k}-\mathbf{q}} + 1)(n_{\mathbf{k}} + n_{\mathbf{q}} + 1)\Big) \\ & + 3B_{\mathbf{k},\mathbf{q}-\mathbf{k}}\Big(n_{\mathbf{q}}(n_{\mathbf{k}} + n_{\mathbf{k}-\mathbf{q}} + 1) + n_{\mathbf{k}-\mathbf{q}} + 1\Big) \\ & + 3B_{\mathbf{q},\mathbf{k}-\mathbf{q}}\, \Big(n_{\mathbf{k}}(n_{\mathbf{q}} + n_{\mathbf{k}-\mathbf{q}} + 1)\Big). \end{aligned} \tag{20}$$

With this truncation, we have established a hierarchy of correlation functions in the terms of the $\hat{\chi}_{\mathbf{k}}$ operators that approximately describes the dynamics of the bosonic gas, provided $n_0 \gg n_{\text{ex}}$, such that connected correlators of higher order have a decreasing magnitude.

IV. THE KINETIC EQUATIONS

In the long-time limit our coupled system of equations (14)–(15) and (17)–(18) reproduce the well-know kinetic equations. This can be seen by formally solving (17) as

$$M_{\mathbf{k},\mathbf{q}}(t) = -ig\sqrt{\frac{n_0}{V}} \int_0^t ds\, F_{\mathbf{k},\mathbf{q}}^{(M)}(s)\, e^{i(\omega_{\mathbf{k}} - \omega_{\mathbf{q}} - \omega_{\mathbf{k}-\mathbf{q}})(s-t)}, \tag{21}$$

and similar for $R_{\mathbf{k},\mathbf{q}}(t)$ in (18). These expressions can now be plugged into (14)–(15), after which we obtain effective dynamics by (i) sending the integration boundary $t \to \infty$ in (21), thus singling out non-oscillating terms in the integrand, and (ii) time averaging over fast oscillations. The result is that the evolution of quasiparticle occupation numbers is governed by the kinetic (or quantum Boltzmann) equations (we drop the superscript $\cdot^{(\chi)}$

for ease of notation)

$$\partial_t n_{\mathbf{k}} = 4\pi \frac{g^2 n_0}{V} \Big\{ \sum_{\mathbf{q}} A^2_{\mathbf{q},\mathbf{k}-\mathbf{q}} \Big(n_{\mathbf{k}-\mathbf{q}} n_{\mathbf{q}} - n_{\mathbf{k}}(n_{\mathbf{q}} + n_{\mathbf{k}-\mathbf{q}} + 1) \Big) \times \delta\big(\omega_{\mathbf{k}} - \omega_{\mathbf{q}} - \omega_{\mathbf{k}-\mathbf{q}}\big) + 2 \sum_{\mathbf{q}} A^2_{\mathbf{k},\mathbf{q}-\mathbf{k}} \Big(n_{\mathbf{q}}(n_{\mathbf{k}} + n_{\mathbf{k}-\mathbf{q}} + 1) - n_{\mathbf{k}} n_{\mathbf{k}-\mathbf{q}} \Big) \times \delta\big(\omega_{\mathbf{q}} - \omega_{\mathbf{k}} - \omega_{\mathbf{k}-\mathbf{q}}\big) \Big\}. \tag{22}$$

Within this approximation, the oscillation frequencies from the evolution of $M_{\mathbf{k},\mathbf{q}}$ have been translated into δ-functions imposing energy conservation for the redistribution of quasiparticle occupation numbers. In our method, the kinetic equations come as a limiting behavior, so that deviations from them can be studied quantitatively; this to our knowledge has not been done previously in 3D.

With (22), we rederive the kinetic equation that is known from the literature on Beliaev-Landau scattering, where it is commonly established with Fermi golden rule [25]. The first term represents the redistribution of quasiparticles through Beliaev decay, where a quasiparticle with high momentum $\mathbf{k}$ decays into (or is formed from) two with $\mathbf{q}$ and $\mathbf{k} - \mathbf{q}$. The second term, in turn, describes the absorption (or emission) of the quasiparticle with momentum $\mathbf{k}$ by a quasiparticle $\mathbf{q} - \mathbf{k}$ (or $\mathbf{q}$). Notice that the second term comes with an additional factor 2 from the two possible scattering channels [21]. See Fig. 1(b) for the corresponding diagrams.

Through the same analysis, we obtain the evolution of pair correlations in the frame rotating with Bogoliubov frequency $2\omega_k$,

$$\partial_t \tilde{c}_{\mathbf{k}} = -4\pi \frac{g^2 n_0}{V} \Big\{ \sum_{\mathbf{q}} A^2_{\mathbf{q},\mathbf{k}-\mathbf{q}} \Big((n_{\mathbf{q}} + n_{\mathbf{k}-\mathbf{q}} + 1)\tilde{c}_{\mathbf{k}} + \tilde{c}_{\mathbf{q}} \tilde{c}_{\mathbf{k}-\mathbf{q}} \Big) \times \delta\big(\omega_{\mathbf{k}} - \omega_{\mathbf{q}} - \omega_{\mathbf{k}-\mathbf{q}}\big) + 2 \sum_{\mathbf{q}} A^2_{\mathbf{k},\mathbf{q}-\mathbf{k}} \Big(\tilde{c}_{\mathbf{q}} \tilde{c}^*_{\mathbf{q}-\mathbf{k}} + (n_{\mathbf{k}-\mathbf{q}} - n_{\mathbf{q}})\tilde{c}_{\mathbf{k}} \Big) \times \delta\big(\omega_{\mathbf{q}} - \omega_{\mathbf{k}} - \omega_{\mathbf{k}-\mathbf{q}}\big) \Big\}, \tag{23}$$

where we see the same δ-functions of energy conservation as in (22). Close to equilibrium, it is enlightening to notice that Eq. (23) reduces to

$$\partial_t \tilde{c}_{\mathbf{k}} \approx -2\gamma^{\mathrm{B}}_{\mathbf{k}}\, \tilde{c}_{\mathbf{k}} - 2\gamma^{\mathrm{L}}_{\mathbf{k}}\, \tilde{c}_{\mathbf{k}}, \tag{24}$$

where $\gamma^{\mathrm{B}}_{\mathbf{k}}$ and $\gamma^{\mathrm{L}}_{\mathbf{k}}$ are the decay rates of a phonon with momentum $\mathbf{k}$ under Beliaev decay and Landau scattering respectively [21]. In fact, Eq. (23) is more general as it also includes nonlinear terms $\sim \tilde{c}_{\mathbf{q}}\tilde{c}_{\mathbf{q}'}$ that accelerate the decay of $\tilde{c}_{\mathbf{k}}$ by incoherent scattering of excitations from the reservoir of modes $\mathbf{q}$ into mode $\mathbf{k}$.

A further quantitative check of the validity of the kinetic model can be done to explicitly show a comparison

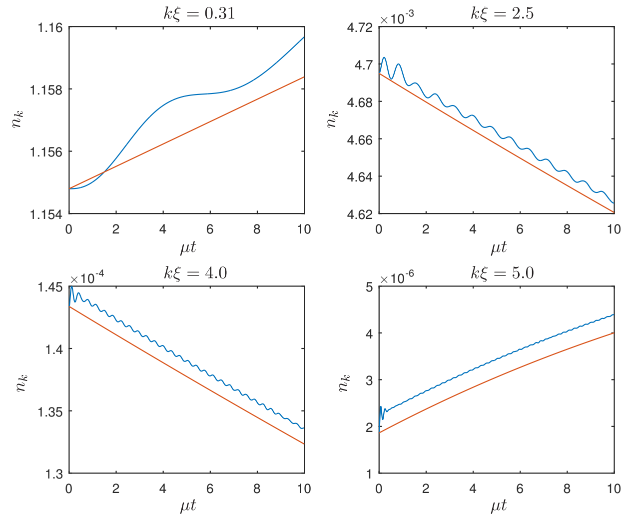

Figure 3. A comparison of the quasiparticle occupation numbers $n_{\mathbf{k}}$ as produced by the integration of the hierarchy of correlation functions (blue lines) and the derived kinetic equation in the adiabatic limit (red lines) for the quench $g_i = 0 \to g_f = 0.05\mu\xi^3$ (corresponding to $n\xi^3 = 20$) in $\tau_s = 0.5\mu^{-1}$ (see initial momentum distribution on Fig. 2). At low momenta, we notice a significant difference between the two predictions. At high momenta, however, the two results lie close to each other and the HOC produces a fast initial oscillation that then dephases, justifying the application of the kinetic description from right after the quench when short distances are considered. We used $N_k = 128$ and $N_c = 200$ with $k_{\max} = 10/\xi$.

between the full integration of the truncated hierarchy and the approximate kinetic description (22)–(23). In Fig. 3, we show the evolution of the quasiparticle occupation numbers for a comparison between the hierarchy of correlation functions and the kinetic equations at short times $\sim 1/\mu$. We observe that the curve of $n_k(t)$ predicted by the kinetic equation differs in two distinct ways from that of the hierarchy: (i) the evolution at very short times is not well captured by the kinetic equation, which results in a small offset (controlled by the interaction strength na_s^3) between the two curves, conserved all along the evolution and (ii) contrary to the kinetic description, the hierarchy of correlations retains high-frequency components in $n_k(t)$. Those two differences are directly related to the two approximations on which kinetic equations are based: (i) they are valid only at long times and (ii) they are valid only on average over a time $\gg 1/\omega_k$.

This analysis shows that for times $\sim 1/\mu$ the kinetic equations show deviations at low wave numbers ($k \ll 1/\xi$). Conversely, higher momentum modes ($k \gtrsim 1/\xi$) allow for an accurate description in terms of a kinetic formulation of the problem.

In the long-time limit, we find that (22) and (23) converge to the values in a thermal ensemble. The momentum distribution of quasiparticles approaches the Bose-Einstein distribution

$$n_{\mathbf{k}}^{\text{th}} = \frac{1}{e^{\beta\omega_{\mathbf{k}}} - 1}, \tag{25}$$

with $\beta = 1/k_B T$ the inverse temperature set by the total injected energy, while the anomalous correlations vanish. The energy after the quench on the level of the quadratic Hamiltonian, $E = E_0 + \sum_{\mathbf{k}} \omega_k \, n_k^{(\chi)}$, is conserved under the kinetic equations. However, from (13) one notices an ultraviolet divergence in the limit of zero switching time. Therefore, introducing a finite switching time sets an effective cutoff in energy, with scaling $E - E_0 \propto \sqrt{\tau_s^{-1}}$. This enables us to fix the total injected energy with the switching time τ_s and, consequently, the final equilibrium temperature of the gas by matching this energy with the energy of a thermal ensemble. When $k_B T > \mu$, we have that $E - E_0 \propto T^{5/2}$, such that we derive the asymptotic scaling $T \propto \tau_s^{-1/5}$. In Fig. 2(b), we show the full variation of equilibrium temperature with switching time τ_s.

V. THE DENSITY-DENSITY CORRELATION FUNCTION

Finally, we investigate the behavior of macroscopic observables in real space, which are expected to exhibit the two distinct relaxation stages. We concentrate on distances of the order of the thermal wavelength $2\pi/k_{\text{th}}$, with $\omega_{k_{\text{th}}} = k_B T$. We choose $\tau_s^{-1} = 0.5\mu$, such that $k_B T = 0.67\mu$ and therefore the thermal wavelength is of the same order as the healing length ξ. For these distances, we can apply the kinetic equations at all times, since they are valid almost instantly after the quench, see Fig. 3.

The first relaxation stage of local observables to their prethermal value is caused by a dephasing mechanism where all $\mathbf{k}$-modes interfere desructively. We therefore define the annihilation operator in position space $\hat{a}(\mathbf{r}) = 1/\sqrt{V} \sum_{\mathbf{k}} e^{i\mathbf{k}\cdot\mathbf{r}} \hat{a}_{\mathbf{k}}$. Our analysis is now focused on the evolution of the density-density correlation function, defined as $g^{(2)}(\mathbf{r} - \mathbf{r}'; t) = \langle : \hat{n}(\mathbf{r}) \, \hat{n}(\mathbf{r}') : \rangle_t / \langle \hat{n}(\mathbf{r}) \rangle_t^2$ for a homogeneously distributed gas, where ':' denotes normal ordering and $\hat{n}(\mathbf{r}) = \hat{a}^\dagger(\mathbf{r})\hat{a}(\mathbf{r})$ is the local density operator. The density-denstiy correlation function has proven its importance previously in the context of analog gravity [31, 32], where the correlation pattern shows a fingerprint of the analog of Hawking radiation at an acoustic black hole's horizon [33].

On the Gaussian level, the density correlation function can be simplified to

$$g^{(2)}(\mathbf{r} - \mathbf{r}'; t) = 1 + \frac{2}{n_0}\big(\mathfrak{n}(\mathbf{r} - \mathbf{r}'; t) + \text{Re}\{\mathfrak{m}(\mathbf{r} - \mathbf{r}'; t)\}\big), \tag{26}$$

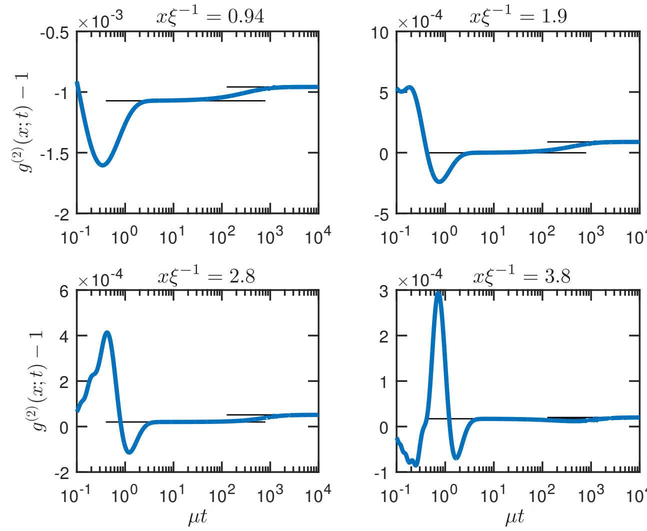

Figure 4. The evolution of the density correlation function after the quench $g_i = 0 \to g_f = 0.05\mu\xi^3$ in $\tau_s = 0.5\mu^{-1}$ (see red line in Fig. 2 for initial momentum distribution) for varying distance $x = |\mathbf{r} - \mathbf{r}'|$, with $\xi = 1/\sqrt{m\mu}$ the healing length. The dashed lines indicate the asymptotic values for the prethermal and thermal (quasi)stationary ensemble; the temperature $T = 0.67\mu$ is found from the initial state. At short distances, we clearly notice a relaxation to a prethermal plateau on a time scale of the order of $\tau_{\text{preth}} = \mu^{-1}$ (for ramps $\tau_s \sim \mu^{-1}$ and $x \sim \xi$), this is due to a dephasing mechanism in $\hat{H}_2$. In $g^{(2)}(x;t)$, this is manifested as a fast oscillation at short times, which then diminishes due to a destructive interference between all $\mathbf{k}$-modes once the light-cone correlation peak has moved away from the considered distance x [16]. Then, at much later times, $\tau_{\text{therm}} \sim 10^3\mu^{-1}$, a new equilibrium value is found that corresponds to the value in the thermal ensemble through the much slower dynamics of $\hat{H}_3$. The difference between the prethermal and thermal value vanishes for increasing separation x as the correlation function drops to zero in this limit. Here, $N_k = 8192$ and $k_{\text{max}} = 10/\xi$ are used, the scattering angle is fixed from energy conservation in the kinetic approximation.

where we defined

$$\mathfrak{n}(\mathbf{r} - \mathbf{r}'; t) = \langle \hat{a}^\dagger(\mathbf{r})\hat{a}(\mathbf{r}')\rangle_t = \frac{1}{V}\sum_{\mathbf{k}\neq 0} e^{i\mathbf{k}\cdot(\mathbf{r}-\mathbf{r}')} n_{\mathbf{k}}^{(a)}(t), \tag{27}$$

and analogous for $\mathfrak{m}(\mathbf{r} - \mathbf{r}') = \langle \hat{a}(\mathbf{r})\hat{a}(\mathbf{r}')\rangle$. The quadratic correlations of fluctuations, $n_{\mathbf{k}}^{(a)}$ and $c_{\mathbf{k}}^{(a)}$, can be obtained from the quasiparticle correlations $n_{\mathbf{k}}^{(\chi)}$ and $c_{\mathbf{k}}^{(\chi)}$ through the inverse of the transformation (11)–(12).

In Fig. 4 we show the evolution of the density correlation function after a ramp $g_i = 0 \to g_f = 0.05\mu\xi^3$ (so that $na_s^3 = 1.3 \cdot 10^{-5}$) at different distances $x = |\mathbf{r} - \mathbf{r}'|$. We observe a clear first relaxation, approximately to the prethermal value on a time scale $\tau_{\text{preth}} \sim \mu^{-1}$ after an initial oscillation due to the light-cone peak [16, 34] that dies out due to dephasing once this has traveled away; this is governed by $\hat{H}_2$. At much longer times, the scatterings contained in $\hat{H}_3$ cause a new relaxation, this time to the thermal value. We find that the thermalization time $\tau_{\text{therm}} \sim 10^3\mu^{-1}$ is in qualitative agreement with the Beliaev-Landau lifetime of the thermal wavenumber $1/\gamma^{BL}_{k_{\text{th}}} \sim 1/\mu\sqrt{na_s^3}$ for $k_BT \sim \mu$ [25].

VI. CONCLUSIONS

We have illustrated that the crossover from a prethermalized to a thermalized state can be witnessed in a cold atomic gas by probing the density correlations after a sudden interaction ramp. The switching time of the ramp determines the final temperature in the equilibrium ensemble. While a simple dephasing mechanism, treated on the level of the quadratic Hamiltonian, causes local observables to relax to a prethermal value, a more sophisticated approach is needed to describe the thermalization stage. Here, third-order interaction processes, known as Beliaev-Landau collisions, are the predominant mechanism to lead the system away from integrability and, therefore, to thermal equilibrium. When focusing on length scales on the order of the thermal wavelength, a kinetic description is sufficient to describe the final relaxation. In principle, our predictions are within reach of current experiments with ultracold atomic gases.

ACKNOWLEDGMENTS

MVR gratefully acknowledges support in the form of a Ph. D. fellowship of the Research Foundation - Flanders (FWO) and hospitality at the BEC Center in Trento. HK is supported by the FWO and the European Union H2020 program under the MSC Grant Agreement No. 665501. MW acknowledge financial support from the FWO-Odysseus program. IC was funded by the EU-FET Proactive grant AQuS, Project No. 640800, and by Provincia Autonoma di Trento, partially through the project "On silicon chip quantum optics for quantum computing and secure communications (SiQuro)".

[1] J. M. Deutsch, Physical Review A **43**, 2046 (1991).
[2] M. Srednicki, Physical Review E **50**, 888 (1994).
[3] M. Rigol, V. Dunjko, and M. Olshanii, Nature **452**, 854 (2008).
[4] M. Rigol, Physical Review A **80**, 053607 (2009).
[5] M. Rigol, V. Dunjko, V. Yurovsky, and M. Olshanii, Physical review letters **98**, 050405 (2007).
[6] T. Langen, S. Erne, R. Geiger, B. Rauer, T. Schweigler, M. Kuhnert, W. Rohringer, I. E. Mazets, T. Gasenzer, and J. Schmiedmayer, Science **348**, 207 (2015).
[7] T. Kinoshita, T. Wenger, and D. S. Weiss, Nature **440**, 900 (2006).
[8] J.-S. Caux and F. H. Essler, Physical review letters **110**, 257203 (2013).
[9] J. Berges, S. Borsányi, and C. Wetterich, Phys. Rev. Lett. **93**, 142002 (2004).
[10] B. Bertini, F. H. Essler, S. Groha, and N. J. Robinson, Physical review letters **115**, 180601 (2015).
[11] M. Buchhold, M. Heyl, and S. Diehl, Phys. Rev. A **94**, 013601 (2016).
[12] C. Chin, R. Grimm, P. Julienne, and E. Tiesinga, Reviews of Modern Physics **82**, 1225 (2010).
[13] C.-L. Hung, V. Gurarie, and C. Chin, Science , 1237557 (2013).
[14] J.-C. Jaskula, G. B. Partridge, M. Bonneau, R. Lopes, J. Ruaudel, D. Boiron, and C. I. Westbrook, Phys. Rev. Lett. **109**, 220401 (2012).
[15] S. S. Natu and E. J. Mueller, Physical Review A **87**, 053607 (2013).
[16] I. Carusotto, R. Balbinot, A. Fabbri, and A. Recati, The European Physical Journal D **56**, 391 (2010).
[17] G. Menegoz and A. Silva, Journal of Statistical Mechanics: Theory and Experiment **2015**, P05035 (2015).
[18] A. Rançon and K. Levin, Physical Review A **90**, 021602 (2014).
[19] S. Beliaev, Sov. Phys. JETP **34**, 299 (1958).
[20] L. Pitaevskii and S. Stringari, Physics Letters A **235**, 398 (1997).
[21] S. Giorgini, Physical Review A **57**, 2949 (1998).
[22] F. Chevy, V. Bretin, P. Rosenbusch, K. W. Madison, and J. Dalibard, Phys. Rev. Lett. **88**, 250402 (2002).
[23] N. Katz, J. Steinhauer, R. Ozeri, and N. Davidson, Physical review letters **89**, 220401 (2002).
[24] For a weakly depleted condensate and a convex Bogoliubov branch, the dynamics of $\hat{H}_3$ largely dominates over that of the fourth order [35].
[25] A. Sinatra, Y. Castin, and E. Witkowska, Physical Review A **80**, 033614 (2009).
[26] We perform a simplified approach, where the number of particles is not conserved, but number-conserving approaches [36] would result in exactly the same Hamiltonians $\hat{H}_2$ and $\hat{H}_3$ [25].
[27] V. Dodonov, Physica Scripta **82**, 038105 (2010).
[28] S. Koghee and M. Wouters, Physical review letters **112**, 036406 (2014).
[29] C. Wilson, G. Johansson, A. Pourkabirian, M. Simoen, J. Johansson, T. Duty, F. Nori, and P. Delsing, Nature **479**, 376 (2011).
[30] N. P. Proukakis, Journal of Physics B: Atomic, Molecular and Optical Physics **34**, 4737 (2001).
[31] R. Balbinot, A. Fabbri, S. Fagnocchi, A. Recati, and I. Carusotto, Physical Review A **78**, 021603 (2008).
[32] I. Carusotto, S. Fagnocchi, A. Recati, R. Balbinot, and A. Fabbri, New Journal of Physics **10**, 103001 (2008).
[33] J. Steinhauer, Nature Physics **12**, 959 (2016).
[34] P. Calabrese and J. Cardy, Journal of Statistical Mechanics: Theory and Experiment **2005**, P04010 (2005).
[35] L. Pitaevskii and S. Stringari, *Bose-Einstein condensation and superfluidity*, Vol. 164 (Oxford University Press, 2016).
[36] Y. Castin and R. Dum, Physical Review A **57**, 3008 (1998).